Published in final edited form as:
Immunity. 2013 March 21; 38(3): 581–595. doi:10.1016/j.immuni.2013.01.009.

Luminal Bacteria Recruit CD103$^+$ Dendritic Cells into the Intestinal Epithelium to Sample Bacterial Antigens for Presentation

Julia Farache[1], **Idan Koren**[1], **Idan Milo**[1], **Irina Gurevich**[1], **Ki-Wook Kim**[1,3], **Ehud Zigmond**[1], **Glaucia C. Furtado**[2], **Sergio A. Lira**[2], and **Guy Shakhar**[1,*]

[1]Department of Immunology, Weizmann Institute of Science, Rehovot 76100, Israel

[2]Immunology Institute, Mount Sinai School of Medicine, New York, NY 10029, USA

SUMMARY

CD103$^+$ dendritic cells (DCs) carry bacteria from the small intestine and can present antigens to T cells. Yet they have not been recorded sampling luminal bacteria or presenting bacterial antigens in mesentery lymph nodes. We used 2-photon microscopy in live Cx3cr1$^{+/gfp}$ × Cd11c-YFP mice to study these processes. At steady state, sparse CD103$^+$ DCs occupied the epithelium. They patrolled among enterocytes while extending dendrites toward the lumen, likely using tight-junction proteins to penetrate the epithelium. Challenge with Salmonella triggered chemokine- and toll-like receptor (TLR)-dependent recruitment of additional DCs from the lamina propria (LP). The DCs efficiently phagocytosed the bacteria using intraepithelial dendrites. Noninvasive bacteria were similarly sampled. In contrast, CD103$^+$ DCs sampled soluble luminal antigen inefficiently. In mice harboring CD103$^+$ DCs, antigen-specific CD8 T cells were subsequently activated in MLNs. Intestinal CD103$^+$ DCs are therefore equipped with unique mechanisms to independently complete the processes of uptake, transportation, and presentation of bacterial antigens.

INTRODUCTION

To initiate adaptive immunity against enteric pathogens and to maintain tolerance toward commensal flora and food antigens (Ags), dendritic cells (DCs) acting as professional antigen-presenting cells (APCs) must survey the intestinal contents and deliver intestinal Ag to mesenteric lymph nodes (MLNs) (Coombes and Powrie, 2008; Rescigno, 2010; Varol et al., 2010; Scott et al., 2011).

*Correspondence: shakhar@weizmann.ac.il.
[3]Present address: Department of Microbial Pathogenesis, Boyer Center for Molecular Medicine, Yale University School of Medicine, New Haven, CT 06510, USA

SUPPLEMENTAL INFORMATION

Supplemental Information includes four figures, Supplemental Experimental Procedures, and ten movies and can be found with this article online at http://dx.doi.org/10.1016/j.immuni.2013.01.009.

A seminal study by Rescigno et al. (2001) has demonstrated that $CD11c^+$ cells, believed to be DCs, send transepithelial dendrites (TEDs) from the lamina propria (LP) that penetrate through tight junctions and capture *Salmonella* from the lumen. It since has been recognized that the LP contains two developmentally-distinct populations of $CD11c^+$ mononuclear phagocytes: $CD11c^{hi}$ $CD103^+$ $CD11b^+$ CX_3CR1^- cells and $CD11c^{int}$ $CD103^-$ $CD11b^+$ CX_3CR1^+ cells (Bogunovic et al., 2009; Schulz et al., 2009; Varol et al., 2009). Of these, $CD103^+$ cells are considered true DCs (Jaensson et al., 2008; Bogunovic et al., 2009; Schulz et al., 2009), whereas CX_3CR1^+ cells are now commonly thought to be resident macrophages (Persson et al., 2010; Varol et al., 2010).

$CD103^+$ DCs seem more adept than CX_3CR1^+ macrophages at coordinating adaptive immunity against gut Ags: They express the chemokine receptor CCR7, allowing them to migrate to MLNs (Jaensson et al., 2008; Bogunovic et al., 2009; Schulz et al., 2009) carrying Ags from gut-encountered bacteria (Bogunovic et al., 2009). At the MLN, they excel at imprinting T cells for gut homing (Annacker et al., 2005; Johansson-Lindbom et al., 2005), and, depending whether the context is inflammatory or tolerogenic, either inducing effector T cells (Johansson-Lindbom et al., 2005; Laffont et al., 2010; Semmrich et al., 2012) or regulatory T cells (Annacker et al., 2005; Sun et al., 2007; Coombes and Powrie, 2008; Scott et al., 2011).

Paradoxically, CX_3CR1^+ macrophages, rather than the $CD103^+$ DCs, are the cells that have been consistently observed sampling the intestinal luminal content by extending TEDs (Rescigno et al., 2001; Niess et al., 2005; Chieppa et al., 2006; Vallon-Eberhard et al., 2006; Varol et al., 2009). Moreover, TLR-ligands (Varol et al., 2009) and contact with microbes (Vallon-Eberhard et al., 2006), including *Salmonella*, have been shown to induce TED formation (Chieppa et al., 2006) and do so in a CX_3CR1-dependent manner (Niess et al., 2005; Vallon-Eberhard et al., 2006).

Unlike CX_3CR1^+ macrophages, $CD103^+$ DCs have not been observed extending TEDs, and it remains unclear how they gain access to luminal bacteria. DCs may directly capture only those pathogens that actively invade the epithelium (Niess et al., 2005) or enter through villus M cells (Jang et al., 2004; Vallon-Eberhard et al., 2006). Alternatively, it has been speculated that $CD103^+$ DCs acquire bacterial Ags from CX_3CR1^+ macrophages (Rescigno, 2010; Scott et al., 2011) or extend their own protrusions toward the gut lumen (Chieppa et al., 2006; Rescigno, 2010). If the latter suggestion is true, some $CD103^+$ DCs would have to be located close to the epithelium or inside it, rather than remain confined to the deep LP (Johansson-Lindbom et al., 2005; Schulz et al., 2009).

For uptake of soluble Ags, the molecular mechanisms may be entirely different. CX_3CR1^+ macrophages have been shown to out-perform $CD103^+$ DCs at such uptake and to do so independently of TEDs (Schulz et al., 2009). In contrast, a recent study (McDole et al., 2012), found $CD103^+$ DCs to be superior, relying on interactions with Ag-channeling goblet cells.

In this study, we used intravital 2-photon microscopy in fluorescent reporter mice to study the dynamic response of $CD103^+$ DCs to *Salmonella* challenge and the cellular behavior that

underlies sampling of bacteria and soluble Ag. We found that bacterial challenge recruits $CD103^+$ DCs from the LP into the epithelium, in which they crawl laterally while sending dendrites into the intestinal lumen. Luminal bacteria are captured using these dendrites and their antigens are subsequently presented in the MLNs of mice harboring $CD103^+$ DCs.

RESULTS

At Steady State, Sparse $CD11c^+CX3CR1^-$ Cells Patrol the Intestinal Epithelium

To study dynamic cell behaviors in the small intestines, we developed a protocol for 2-photon microscopy of the luminal aspect of the ileum in live mice. Our procedure minimized peristaltic movement in the externalized tissue, preserved blood flow, and maintained the integrity of the epithelial surface (see Movie S1 available online). Using this protocol, we could observe both the epithelium and the LP for up to 4 hr.

To distinguish between mononuclear phagocytes in vivo, we crossed the *Cd11c*-YFP (Lindquist et al., 2004) and *Cx3cr1*^{gfp} (Jung et al., 2000) mouse strains. In this dual reporter strain, $CD103^+$ DCs are expected to be YFP^+ and GFP^- and appear yellow, whereas CX_3CR1^+ macrophages should be YFP^+ and GFP^+ and appear light-colored.

As expected, 2-photon microscopy recorded highly-elaborate cells which constituted most of the fluorescent cells in the LP and were absent from the epithelium (Figure 1). These cells, consistent with earlier descriptions of CX_3CR1^+ macrophages (Niess et al., 2005; Chieppa et al., 2006; Varol et al., 2009) expressed both CX_3CR1-GFP and CD11c-YFP and their exact hue depended on the ratio of these two fluorescent proteins (Figure 1A). CX_3CR1^+ macrophages showed little lateral displacement, but projected highly-dynamic dendrites within the LP and occasionally in between epithelial cells (Movie S2).

A separate cell population was CD11c-YFP^{int} and CX_3CR1-GFP^- (Figure 1). These large cells displayed amoeboid morphology (Figures 1A and 1B); most resided in the LP (Movie S2), but some, estimated at around 1–2 per villus, occupied the epithelium itself (Figures 1B and 1C; Movie S3). When compared to macrophages in the LP, these cells displayed less than half of the YFP intensity and could therefore easily go unnoticed (Figures 1D and 1E).

$YFP^{int}GFP^-$ cells in the epithelium were motile and meandered, encircling the lateral aspects of epithelial cells, suggesting that they were located above the basal membrane (Figure 1F; Movie S3). Three-dimensional movement analysis recorded a significantly higher displacement rate for these cells over CX_3CR1^+ macrophages (Figure 1G). Based on their morphology, motility, and fluorescence profile, we suspected that these cells were $CD103^+$ DCs.

Isolated $CD103^+$ DCs Show Intrinsic Motility

To test our hypothesis, we first examined the morphology and motility of $CD103^+$ DCs in vitro. By using flow cytometry, we sorted $CD103^+$ mononuclear phagocytes from the ileum and visualized their behavior (Figures 1H–1L; Movie S4). $CD103^+$ DCs displayed amoeboid morphology (Figures 1H and 1J) while spontaneously and vigorously crawling at an average speed of 11 μm/min (Figures 1J and 1L). They extended lamellipodia at the leading edge

and trailed distinct $CD103^+$ uropods behind them (Figure 1J). In contrast, most CX_3CR1^+ macrophages adhered to the plate, displaying stellate morphology and dynamic protrusions but showing little lateral movement (Figures 1I, 1K, and 1L).

CD11c-YFP^{int} Cells Are $CD103^+$ DCs

We proceeded to establish the identity of CD11c-YFP^{int} cells as $CD103^+$ DCs.

First, we excised the small intestine and rapidly fixed it to characterize CD11c-YFP^{int} cells using whole-mount fluorescent immunohistology. Staining with antilaminin indicated that some YFP^+ cells resided directly above the basement membrane among enterocytes (Figure 2A), exhibited intermediate YFP intensity (Figure 2A), and adopted the amoeboid morphology previously recorded using 2-photon microscopy (Figures 2B and 2C). In *Cd11c*-YFP × *Cx3cr1*^{gfp} mice, YFP^+ cells in the epithelium never expressed GFP (Figure 2C). YFP^{int} cells expressed CD11c (Figures 2D, 2E, and 2G) and CD103 (Figures 2F–2H), but not CD4 or CD8 (Figures 2A–2C and 2E and 2F), indicating that they were not intraepithelial lymphocytes (IELs). This was further demonstrated by the presence of YFP^{int} $CD11c^+$ cells in the epithelium of *Rag1*$^{-/-}$ mice (Figure 2I), which lack intraepithelial T cells.

Second, we examined CD11c-YFP^{int} cells using flow cytometry. We harvested the small intestine of *Cd11c*-YFP mice, discarding the Peyer's patches (PPs), and gently separated the LP from the epithelium. As expected, $MHCII^+$ $CD11b^+$ mononuclear phagocytes included two major populations: $CD11c^{hi}CD103^+$ DCs and $CD11c^{int}CD103^-$ cells (Figures 3A and 3B; Figure S1A). In Cx3cr1$^{+/gfp}$ mice, almost all the latter cells were GFP^+ (Figures 3A and 3B), so they are hereafter referred to as CX_3CR1^+ macrophages. Although they expressed more CD11c, $CD103^+$ DCs in the LP, epithelium (Figures 3A and 3B) and MLNs (Figure 3C) displayed lower YFP intensity than CX_3CR1^+ macrophages, corresponding with 2-photon microscopy and immunohistological results.

As noticed before (Bogunovic et al., 2009; Schulz et al., 2009), in the LP, CX_3CR1^+ macrophages outnumbered $CD103^+$ DCs 3- to 4-fold (Figure 3A; Figure S3A). However, in the epithelium, the opposite was true, and $CD103^+$ DCs typically outnumbered CX_3CR1^+ cells (Figure 3B; Figure S3A). Detailed analysis indicated that CX_3CR1^+ macrophages found in epithelial preparations were a contamination from the LP, because these cells crossed the basal membrane during cell separation (Figure S1B; Movie S5) and gradually accumulated in the epithelial cell fraction (Figure S1C).

To examine the relationship between $CD103^+$ DCs located in the epithelium and those in the LP, we compared the activation markers major histocompatibility complex class II (MHC-II), CD40, CD80, and CD86, and the linage markers CD115 (MCSF-R), GR-1, and CD135 (Flt3). The two populations were indistinguishable (Figure S1D) indicating that they did not represent distinct linages of DCs but belong to the same cell pool shared between the two locations.

Third, because CD11c is expressed not only by myeloid cells but also by some lymphoid cells, such as IELs (Huleatt and Lefrançois, 1995) and plasma cells (Hebel et al., 2006), we

verified that we had not mistaken these cells for CD11c-YFP^{int} DCs. For this aim we further characterized the location, brightness, and behavior of CD11c^{+} lymphoid cells.

Flow cytometry analysis of *Cd11c*-YFP mice revealed that about 1% of their IELs were YFP^{lo} (Figure S2A), showing, on average, half the YFP intensity of CD11c-YFP^{int} DCs (Figure S2B). Most of these cells were too dim to identify using 2-photon microscopy (Lindquist et al., 2004), but because IELs dominated the epithelial leukocyte population, the brightest ones could indeed be imaged and appeared smaller and rounder than YFP^{int} DCs (Figures S2C and S2D). Fluorescent immunohistology failed to detect CD4^{+} or CD8^{+} IELs that expressed YFP, confirming their low fluorescence (Figure 2; Figure S2E).

Consistent with previous studies (Hebel et al., 2006), around 20% of intestinal immunoglobulin A (IgA)-producing plasma cells were YFP^{hi} (Figure S2F). These cells, though, were immobile ovoid cells that resided deep in the LP (Figure S2G). No YFP was expressed by other immune cells, including neutrophils, B cells, plasmacytoid DCs, and eosinophils.

Finally, we examined the response of CD11c-YFP^{int} cells to granulocyte macrophage colony-stimulating factor (GM-CSF), which promotes proliferation of intestinal CD103^{+} CD11b^{+} DCs (Bogunovic et al., 2009; Schulz et al., 2009). Two-photon microscopy of mice transplanted with a tumor secreting GM-CSF (Mach et al., 2000) revealed that dynamic GFP^{-}YFP^{int} cells expanded in both the LP and epithelium (Figures 3D–3F; Movie S6). Flow cytometry corroborated this finding (Figure 3G) while immunohistology confirmed that expanded GFP^{-}YFP^{int} cells expressed CD103 (Figure 3H) but not T cell markers (Figure 3I).

Taken together, data from immunohistology, 2-photon microscopy, and flow cytometry strongly suggest that low numbers of CD103^{+} DCs reside at steady state not only in the LP, but also in the epithelium, and that they correspond to GFP^{-} YFP^{int} cells in *Cx3cr1*$^{+/gfp}$ × *Cd11c*-YFP mice. We shall henceforth refer to these cells as CD103^{+} DCs.

Bacterial Challenge Recruits CD103^{+} DCs to the Epithelium

In correspondence with previous research (Rescigno et al., 2001; Niess et al., 2005; Chieppa et al., 2006; Vallon-Eberhard et al., 2006; Arques et al., 2009; Bogunovic et al., 2009; Uematsu and Akira, 2009; Varol et al., 2009), we used *Salmonella typhimurium* to study the response of CD103^{+} DCs to luminal bacteria. We applied χ4550 GFP^{+} *Salmonella* (Yrlid et al., 2001) to the luminal surface. As shown by 2-photon microscopy, within 30 min CD103^{+} DCs were mobilized from the LP, accumulated in the epithelium, and started crawling laterally within it (Figures 4A and 4B; Movie S7). DC recruitment was confirmed by immunohistological analysis (Figure 4C). We used flow cytometry to quantify DC recruitment. Injection of *Salmonella* into the ligated ileum (Rescigno et al., 2001) increased the frequency of CD103^{+} DCs in the epithelium (Figure 4D), raising their absolute numbers from ~2,500 to ~22,000 cells (Figure 4E). DCs were likely recruited from the LP, which experienced a simultaneous decrease in DC frequency. CX_3CR1^{+} macrophages, in contrast, did not mobilize.

Recruitment of CD103$^+$ DCs Likely Depends on TLRs and Chemokines

To better understand molecular cues required for DC recruitment, we investigated signaling pathways downstream of chemokine and Toll-like receptors (TLRs).

We first tested whether TLRs could mediate DC recruitment. To that aim, we examined the intestines of *Myd88*$^{-/-}$ × *Ticam1*$^{-/-}$ double-deficient mice whose TLRs as well as interleukin-1 (IL-1) and IL-18 receptors cannot signal (Yamamoto et al., 2003). Although the steady-state frequency of CD103$^+$ DCs in the LP of *Myd88*$^{-/-}$ × *Ticam1*$^{-/-}$ mice was normal (~1.4% of total cells), it was greatly reduced in the epithelium (Figure 4F). Moreover, *Salmonella* challenge in *Myd88*$^{-/-}$ × *Ticam1*$^{-/-}$ mice failed to recruit more CD103$^+$ DCs from the LP to the epithelium (Figure 4F). To test which cells require TLR signaling for DC recruitment, we produced chimeric mice harboring (wild-type) WT nonhematopoietic cells and *Myd88*$^{-/-}$ × *Ticam1*$^{-/-}$ hematopoietic cells, as well as the reciprocal chimeras. In both groups, *Salmonella* failed to recruit CD103$^+$ DCs (Figure 4F), likely indicating that both DCs and enterocytes need intact signaling cascades for recruitment.

Next we asked whether CD103$^+$ DC recruitment is chemokine-dependent: We systemically treated mice overnight with pertussis toxin (PTx), known to block G protein-mediated (Gαi) signaling and shown to inhibit chemokine-induced migration of leukocytes in vivo (Huang et al., 2007; Fooksman et al., 2010). Although PTx did not reduce the steady-state frequency of CD103$^+$ DCs in the epithelium (Figure 4G) and LP (Figure S3A), it significantly reduced the efficiency of DC recruitment by *Salmonella* (Figure 4G).

Taken together, these data establish that DC recruitment to the epithelium is an active chemokine-driven process that likely requires signaling downstream of MyD88 or TRIF in both DCs and epithelial cells.

A chemokine which might attract CD103$^+$ DCs into the epithelium is CCL20, which is secreted by inflamed intestinal epithelial cells (Izadpanah et al., 2001), acts through the CCR6 receptor, and has been implicated in attracting DCs to the epithelium (Anjuère et al., 2004; Le Borgne et al., 2006; Cruickshank et al., 2009). *Salmonella* infection was shown to induce CCL20 secretion and encourage TED formation (Chieppa et al., 2006). Our analysis indicates that CD103$^+$ DCs express some membranal CCR6 (Figure S3B), but neither CCL20 blockade (Figure S3C) nor deficiency in CCR6 in hematopoietic cells (Figure S3D) prevented their recruitment to the epithelium. Similarly, *Cd103*$^{-/-}$ mice, which lack the αE integrin, had normal numbers of CD11c^{hi} DCs in the epithelium at baseline and following *Salmonella* challenge (Figure S3E), indicating that this integrin, although possibly involved in interactions with enterocytes, is not strictly required for entry into the intra-epithelial space.

CD103$^+$ DCs in the Epithelium Actively Sample Luminal Salmonella

We next assessed whether, following migration to the epithelium, CD103$^+$ DCs sample bacteria from the intestinal lumen.

We first assessed the intrinsic phagocytic capacity of CD103$^+$ DCs in comparison to CX_3CR1^+ macrophages, which are believed to be phagocytic (Rivollier et al., 2012). The

DCs, isolated using flow cytometry and coincubated with *Salmonella* in vitro, proved as phagocytic as macrophages along varying bacterial concentrations (Figure 5A), indicating that they can sample these bacteria directly and efficiently.

To establish whether $CD103^+$ DCs can utilize this capacity in vivo, we imaged the intestine following challenge with GFP^+ *Salmonella*. Observing the luminal aspect of the live ileum 1–2 hr after challenge, we could clearly visualize $CD103^+$ DCs replete with intracellular bacteria (Figure 5B).

To quantify this uptake, we injected a ligated section of the ileum with GFP^+ *Salmonella* and assessed phagocytosis in the LP and epithelium using flow cytometry (Figure 5C; Figure S4A). *Salmonella* first appeared in $CD103^+$ DCs in the epithelium—by 2 hr, 2.4% of $CD103^+$ DCs in this compartment contained bacteria, whereas ingestion in the LP remained negligible. At 5 hr, *Salmonella*$^+$ DCs were also detected in the LP. ImageStream analysis indicated that the bacteria had been internalized (Figure S4B). To ensure that DCs did not pick up unwashed bacteria during cell isolation, we conducted it in the presence of gentamicin (Bowe and Heffron, 1994)—the efficiency of bacterial sampling was not reduced (Figure S4C).

Salmonella Uptake by $CD103^+$ DCs Is an Active Chemokine-Dependent Process

The χ4550 *Salmonella* strain we had used (Yrlid et al., 2001), although attenuated, can attach to the epithelium and invade it (Schödel et al., 1994), potentially engaging $CD103^+$ DCs. We therefore assessed whether $CD103^+$ DCs in the epithelium can sample noninvasive SB161 *Salmonella* from the lumen. This strain can attach to the epithelium but cannot actively cross it due to a nonfunctional TTSS-1 gene (Hapfelmeier et al., 2005). $CD103^+$ DCs sampled this strain as efficiently as they sampled the invasive χ4550 strain (Figure 5D). Correspondingly, intraepithelial $CD103^+$ DCs could sample inert beads (Figure S4D) and were observed accumulating them and traveling back to the LP (Figure S4E).

Because the bacteria did not have to invade the epithelium to be taken up by $CD103^+$ DCs, we hypothesized that bacterial uptake depended on chemokine-directed motility. In agreement with that, overnight treatment with PTx not only reduced $CD103^+$ DCs recruitment to the epithelium (see above) but also severely impaired the ability of those DCs that had reached the epithelium to take up bacteria (Figure 5E).

Intraepithelial DCs Extend Dendrites into the Lumen and Capture Bacteria

While patrolling the epithelium, most $CD103^+$ DCs could be visualized sending dendrites between epithelial cells into the lumen (Figure 5F; Movies S6 and S8). These dendrites differed morphologically from the previously-described TEDs extended by CX_3CR1^+ macrophages (Niess et al., 2005). On the basis of morphometric analysis of 15 DCs, the dendrites had a larger diameter (~4.5 μm versus ~1.8 μm), narrowed toward their tips, and did not terminate in globular structures. On average, each such $CD103^+$ DC extended 6.5 dendrites per hr, retracting them after ~3.5 min. The presence of luminal *Salmonella* did not stimulate more formation of such dendrites.

TED formation by CX_3CR1^+ macrophages did not feature in our intravital preparations as prominently as in previous histological studies (Rescigno et al., 2001; Niess et al., 2005; Vallon-Eberhard et al., 2006; Varol et al., 2009). Although we could occasionally see such protrusions probing between epithelial cells (Movie S8), they were relatively rare, typically did not reach the lumen, and never terminated in globular structures. We could only observe such globular structures in explanted tissue, especially following removal of the epithelium (Figure S1B; Movie S5). Based on morphological considerations, these globular structures may indicate apoptosis (Brokaw et al., 1998).

To retrieve Ags located beyond an epithelial barrier, the dendrites of DCs must breach the tight junctions that seal the epithelial barrier at the luminal surface (Rescigno et al., 2001). To do that, they may be expressing tight junction proteins, as reported for lung $CD103^+$DCs (Sung et al., 2006) and epidermal Langerhans cells (Zimmerli and Hauser, 2007). Indeed, real-time PCR analysis revealed that $CD103^+$ DCs (as well as CX_3CR1^+ macrophages) express the tight junction proteins Claudin-4 and ZO-2 (Figures S4F and S4G).

We proceeded to inspect the cellular mechanism of bacterial sampling directly. $CD103^+$ DCs could be seen sending dendrites across the epithelial cell layer, and engulfing one or two *Salmonella* bacteria in the lumen (Figure 5G). Strikingly, the dendrites of $CD103^+$ DCs rapidly retracted toward the soma after contacting *Salmonella*, bringing the captured bacteria with them (Movie S9).

Intraepithelial $CD103^+$ DCs Capture Soluble Ag from the Lumen

To check whether the intraepithelial position of $CD103^+$ DCs could also facilitate the capture of soluble proteins from the intestinal lumen, we injected an ileal section with fluorescently-labeled ovalbumin prior to flow cytometry analysis. $CD103^+$ DCs in the epithelium were four times more likely to ingest OVA-Alexa-594 Ag than their counterparts in the LP (Figure 6A). However, in accordance with previous results (Schulz et al., 2009), $CX3CR1^+$ macrophages in the LP took up soluble OVA more efficiently than $CD103^+$ DCs —perhaps due to differential expression of scavenger receptors.

To understand whether $CD103^+$ DCs can use their dendrites to sample luminal soluble Ags, we imaged the uptake of OVA-Alexa-594 injected into the lumen. Following injection, rare $CD103^+$ DCs accumulated the Ag inside small endocytic vesicles (Figure 6B) while actively crawling among epithelial cells in the apical villi. Several of these cells could be seen extending dendrites toward the lumen (Figure 6B; Movie S10). No such Ag-containing cells could be located in the LP.

Unlike $CD103^+$ DCs, which rarely took up OVA, the majority of CX_3CR1^+ macrophages ingested the Ag, corroborating our FACs results. OVA quickly concentrated in large cytoplasmic vacuoles inside macrophages (Figure 6C; Movie S10). Some cells could be visualized shuttling the Ag through delicate dendrites toward the soma (Figure 6C; Movie S10, inset), or engulfing large OVA inclusions (Figure 6D).

In accordance with a recent report (McDole et al., 2012), we could observe epithelial cells, morphologically consistent with goblet cells, containing OVA Ag. OVA-containing

CX_3CR1^+ macrophages, however, were dispersed throughout the LP, not necessarily in contact with the epithelium. So, although goblet cells are possible gateways for entry of soluble Ags from the lumen, we have no evidence for direct transfer of these Ags to mononuclear phagocytes in general and to $CD103^+$ DCs in particular.

$CD103^+$ DCs from the Epithelium Can Activate T Cells

Finally, we examined the potential of $CD103^+$ DCs as APCs. Coculture of intraepithelial $CD103^+$ DCs pulsed with ovalbumin protein with OT-I $CD8^+$ T cells, resulted in T cell proliferation (Figure 7A) and in simultaneous upregulation of the gut-tropic $\alpha4\beta7$ integrin (Figure 7B) showing that these cells can potentially participate in cross-presentation and imprinting. In addition, following coculture with *Salmonella* (Figure 7C), $CD103^+$ DCs isolated from the epithelium, but not CX_3CR1^+ macrophages, upregulated the CCR7 receptor, required for migration toward lymphatics (Jang et al., 2006) and into them (Tal et al., 2011). To study the involvement of $CD103^+$ DCs in cross-presentation in vivo, we compared the activation of transferred OT-I T cells in the MLNs of WT mice and *Flt3*$^{-/-}$ mice (Mackarehtschian et al., 1995) which have CX_3CR1^+ macrophages but not $CD103^+$ DCs in the LP (Bogunovic et al., 2009; Varol et al., 2009). Forty hours after OVA-GFP *Salmonella* had been introduced into the gut, OT-I T cells transferred into WT mice become activated, as evidenced by significantly upregulated CD69 compared to controls. In contrast, in *Flt3*$^{-/-}$ mice, no such increase occurred (Figures 7D and 7E).

DISCUSSION

This study observed $CD103^+$ DCs as they patrol the epithelium of the small intestine and capture pathogenic bacteria attaching to its surface. We used 2-photon microscopy in live *Cx3cr1*$^{+/gfp}$ × *Cd11c*-YFP mice to locate a population of GFP^+ YFP^{int} cells that occupied the LP and the epithelium. The small epithelial population consisted of amoeboid cells that crawled, at relatively high speeds, on top of the basal membrane among enterocytes. Their identity as $CD103^+$ DCs was corroborated based on immunohistology and their response to GM-CSF. Flow cytometry data, although it may over-represent $CD103^+$ DC numbers due to contamination from the LP, also supported this identification. The findings demonstrated that YFP^{int} cells were neither $CD11c^+$ lymphocytes nor contaminant cells from the LP. Phenotypically, intraepithelial $CD103^+$ DCs were indistinguishable from those in the LP, indicating that they come from a common cellular pool spanning the two locations. *Salmonella* challenge recruited many more $CD103^+$ DCs to the epithelium but only when both hematopoietic cells and nonhematopoietic cells had functional TRIF and MyD88; likewise, treatment with PTx blocked DC recruitment. Bacteria first appeared inside DCs in the epithelium, where they could be visualized using 2-photon microscopy, and only later in the LP. Sampling was inefficient in mice treated with PTx. The DCs expressed the tight-junction proteins Claudin-4 and ZO-2 and sent thick dendrites through epithelial tight junctions. These dendrites then engulfed *Salmonella* bacteria in the lumen and rapidly retracted toward the soma. $CD103^+$ DCs located in the epithelium, but not in the LP, could also capture soluble protein from the lumen, but did so less efficiently than CX_3CR1^+ macrophages. As indications that they can act as APCs, following maturation, intraepithelial $CD103^+$ DCs upregulated CCR7, induced proliferation of Ag-specific $CD8^+$ T cells and

imprinted them for gut homing. Correspondingly, intraluminal *Salmonella* activated Ag-specific T cells in the MLNs of WT mice, but not *Flt3*$^{-/-}$ mice, which lack intestinal CD103^{+} DCs.

These observations suggest a likely scenario for the interaction between CD103^{+} DCs and intraluminal bacteria: At steady state, most CD103^{+} DCs inhabit the LP, but sparse cells patrol the epithelium, maintained there by TLR signaling from the intestinal flora. The cells glide on the basement membrane below the tight junction layer. When bacteria attach to the luminal surface, CD103^{+} DCs capture them in a two-step process. First, enterocytes and sentinel DCs sense bacteria-derived TLR ligands and secrete chemokines to rapidly recruit more LP CD103^{+} DCs to the epithelium. Second, while patrolling this space, the newly-arrived DCs extend dendrites toward the lumen, relying on tight junction proteins to penetrate the tight junctions. The dendrites extend in response to chemokines and rapidly engulf bacteria. CD103^{+} DCs then upregulate CCR7, return to the LP, and emigrate through lymphatics to the draining MLNs, where they present the captured Ags to T cells.

Our findings place CD103^{+} DCs, armed with suitable cellular behavior, at an advantageous position to efficiently sample luminal Ags. For this task, they require assistance from neither CX_3CR1^{+} macrophages nor villous M cells. We thus suggest that CD103^{+} DCs can independently carry out the entire process of Ag uptake, transportation, and presentation.

Although we have not followed intraepithelial CD103^{+}CD11b^{+} DCs as they migrate through lymphatics, their role in delivering pathogenic *Salmonella* to the MLNs has been demonstrated before (Bogunovic et al., 2009). Using a similar approach, we further showed that *Flt3*$^{-/-}$ mice lacking CD103^{+} DCs show a poor CD8 T cell response in the MLNs against antigen from *Salmonella*. CD103^{+} DCs, therefore, may out-perform CX_3CR1^{+} macrophages not only in pathogen delivery, but also in inducing adaptive immune response against acute enteric infections. However, under chronic inflammation (Zigmond et al., 2012), or dysbiosis (Diehl et al., 2013), other mononuclear phagocytes make take over this role.

Whether CD103^{+} DCs would lose their intrinsic tolerogenic nature during *Salmonella* infection to become potent inflammatory APCs is still an open question. Nonetheless, complementary pathways that involve bacterial transcytosis through M cells in PPs (Jones et al., 1994) and isolated lymphoid follicles (Halle et al., 2007) are probably the ones to deliver most of the luminal *Salmonella* into DCs and likely contributed to the in vivo T cell activation we have observed. Transfer of particulate bacteria through goblet cells is less likely, because these cells failed to transfer large proteins and beads into the lumen (McDole et al., 2012).

Unlike the lung, where CD103^{+} DCs maintain close association with the basolateral side of bronchial epithelial cells (Sung et al., 2006), previous studies of the gut have concluded that CD103^{+} DCs are located deeper in the LP than CX_3CR1 macrophages (Johansson-Lindbom et al., 2005; Schulz et al., 2009). Others, though, reported that CD103^{+} DCs amount to a third of the CD11c^{+} cells in the epithelium (Bogunovic et al., 2009) and could locate them in histological sections of the jejunum (McDonald et al., 2012). MHC-II^{+} DCs could also be

identified in the epithelium of the rat colon and jejunum (Maric et al., 1996). In agreement with these latter studies, we show that, even at steady state, $CD103^+$ DCs occupy the epithelium and crawl among enterocytes. Electron microscopy of the basement membrane of the intestinal villi has revealed pores through which lymphocytes and macrophages sent protrusions or trafficked (Takahashi-Iwanaga et al., 1999). $CD103^+$ DCs may thus take advantage of these pores to migrate from the LP to the epithelium and back.

Although several groups have imaged the small intestine of *Cd11c*-YFP mice (Schulz et al., 2009; McDole et al., 2012), they have not identified this YFP^{int} DC population within the epithelium. The cells may have been missed because, at 1–2 cells per villus, they are relatively rare under steady-state conditions, and because they are dim, expressing ~2.5 times less YFP than nearby CX_3CR1^+ macrophages.

A recent study by McDole et al. (2012) used *Cx3cr1*$^{+/gfp}$ × *Cd11c*-YFP mice and equated $CD103^+$ DCs with a population of YFP^{hi} GFP^{lo} cells imaged in the LP. These cells appeared to form the majority of YFP^+ cells in the LP, and sampled luminal Ag more efficiently. This finding, however, is at odds with previous literature showing that $CD103^+$ DCs are outnumbered 3 to 1 by CX_3CR1^+ macrophages in the LP (Bogunovic et al., 2009; Schulz et al., 2009; Kinnebrew et al., 2012), and are poor at OVA uptake (Schulz et al., 2009). Here we have directly shown that YFP^{hi} cells in these reporter mice are actually CX_3CR1^+ macrophages.

Surprisingly, our imaging and flow cytometry findings show that although they express the highest amounts of membranal CD11c, $CD103^+$ DCs in the LP, epithelium and MLNs show intermediate YFP intensity. Perhaps the longer turnover of CX_3CR1^+ macrophages (Jaensson et al., 2008; Schulz et al., 2009) allows them to accumulate more YFP. Alternatively, the $CD103^+$ DCs may require additional transcriptional control elements to strongly express YFP. Similarly, intestinal plasmacytoid DCs in *Cd11c*-YFP mice do not express any YFP, even though they express some CD11c (Nakano et al., 2001).

The presence of $CD103^+$ DCs in the epithelium, rather than only in the LP, could solve two puzzles: First, in vitro studies suggest that DCs are conditioned by epithelial cells to express RALDH2 (Iliev et al., 2009), and so produce abundant retinoic acid (Iwata et al., 2004), a molecule critical for shaping the homing patterns and cell fate of intestinal T lymphocytes (Mucida et al., 2007; Sun et al., 2007; Coombes and Powrie, 2008). The intimate DC-epithelial contacts that we have demonstrated would allow direct conditioning of $CD103^+$ DCs, as recently suggested (McDonald et al., 2012). Second, epithelial location would explain why intestinal DCs express their hallmark membranal marker—CD103. This molecule, also known as the αE integrin subunit, couples with the β7 chain to form the αEβ7 integrin (Parker et al., 1992). In this capacity it binds E-cadherin (Cepek et al., 1994), an adhesion molecule found on the basolateral membranes of epithelial cells (Boller et al., 1985; Hermiston and Gordon, 1995). CD103 expression, together with the tight junction proteins Claudin-4 and ZO-2, could assist DCs in navigating among enterocytes and sending dendrites through their connecting junctions. Indeed, a role for CD103 in dendrite formation has been established in epidermal T cells (Schlickum et al., 2008). Our studies in *Cd103*$^{-/-}$ mice, though, did not find this molecule to be essential for DC recruitment to the epithelium.

Previously, *Salmonella* was shown to trigger the formation of TEDs by mononuclear macrophages; the cells themselves remained in the LP (Rescigno et al., 2001; Niess et al., 2005; Chieppa et al., 2006). Here in contrast, the bacteria recruited the entire cell bodies of $CD103^+$ DCs into the epithelium. The processes sent by these DCs are "intraepithelial," rather than "transepithelial" dendrites. Although the latter may exist, true TEDs sent by $CD103^+$ DCs are unlikely contributors to bacterial sampling. Indeed, within 2 hr of *Salmonella* injection, LP DCs phagocytosed negligible numbers of bacteria (Figure 5C; Figure S7A). This suggests that, as a rule, to gain access to luminal bacteria, DCs must first perform "step 1"—recruitment—before going through "step 2"—sampling.

Correspondingly, mononuclear phagocytes have been recorded in the epithelium before: CX_3CR1^+ cells migrated unidirectionally into the lumen of the small intestine following infection with flagellated *Salmonella* (Arques et al., 2009); DCs were shown to populate the colonic epithelium following infection with *Trichuris muris* (Cruickshank et al., 2009); most pertinently, DCs whose marker profile is consistent with $CD103^+$ DCs were found in the epithelium of the small intestine after oral administration of cholera toxin (Anjuère et al., 2004).

It remains to be seen which specific TLR ligands, expressed by *Salmonella* or released by it, recruit $CD103^+$ DCs into the epithelium. These DCs were shown to express TLR5 and TLR9, but not TLR2, TLR3, TLR4, or TLR7 (Uematsu et al., 2006, 2008; Fujimoto et al., 2011; Kinnebrew et al., 2012). Notably, TLR5 deficiency impaired the transport of *Salmonella* from the intestinal tract to MLNs (Uematsu et al., 2006), raising the possibility that migratory DCs might require TLR5 to sample *Salmonella*. The epithelial cells of the small intestine express a wider variety of TLRs (Abreu, 2010), including TLR1 through TLR9 and TLR11, and the engagement of these receptors may trigger the recruitment of $CD103^+$ DCs, much like LPS triggers the extension of TEDs in the distal ileum (Chieppa et al., 2006).

This division of labor may explain our finding using bone marrow transfer: To recruit $CD103^+$ DCs to the epithelium, both hematopoietic cells (likely DCs) and nonhematopoietic cells (likely enterocytes) had to possess intact MyD88 and TRIF signaling. This finding suggests a cascade of events in which cells exposed to the luminal content (e.g., enterocytes or Paneth cells) recognize the bacteria through TLRs and induce local inflammation through cytokines, such as IL-1 and IL-18, whose receptors are MyD88-depndent (Adachi et al., 1998).

The end-result of Ag presentation by $CD103^+$ DCs, be it tolerogenic (Coombes et al., 2007; Sun et al., 2007) or immunogenic (Laffont et al., 2010), depends on the context of Ag uptake (Laffont et al., 2010; Scott et al., 2011; Semmrich et al., 2012). Ultimately, manipulating the access of $CD103^+$ DCs to bacterial Ag, as we crudely did here, could relieve inflammatory bowel disease or boost oral vaccination. Better understanding of the molecular mechanisms that allow these DCs to sample luminal Ags and means to specifically target these cells in vivo would be needed before this becomes a viable option.

EXPERIMENTAL PROCEDURES

Mice

Strains used were as follows: C57BL/6 *Cd45.2*, *Cd11c-YFP*, *Cx3cr1*$^{gfp/+}$, *Actin-Cfp*, *MyD88*$^{-/-}$ × *Ticam1*$^{-/-}$, *Ccr6*$^{-/-}$, *Cd103*$^{-/-}$, OT-I, and *Flt3*$^{-/-}$. Bone marrow chimeras were produced by irradiation at 950 rad and transfer of 3 × 10^6 bone marrow cells. Mice were maintained in specific pathogen-free conditions and handled according to protocols approved by the Weizmann Institute Animal Care Committee.

GM-CSF Treatment

Mice were injected subcutaneously (s.c.) with 4 × 10^6 B16 tumor cells expressing GM-CSF (Mach et al., 2000) and analyzed 2 weeks later.

Isolation of Intestinal Cells

The ileum was resected and separated from PPs. Cells were released from the epithelium by rotation for 15 min at 37°C with 5 mM EDTA. LP cells were released after further 45 min incubation with collagenase-D and DNase.

Bacterial Strains

The following strains of *Salmonella typhimurium* were used: χ4550 expressing or not expressing OVA-GFP (Yrlid et al., 2001) and noninvasive SB161 (Hapfelmeier et al., 2005).

In Vitro Phagocytosis Assay

We isolated 2 × 10^6 cells from the LP, cocultured them with GFP$^+$ *Salmonella* for 1 hr at 37°C, treated them with 500 μg/ml gentamicin for 60 min, and washed them for flow cytometric analysis.

Analysis of T Cell Proliferation

CD103$^+$ DCs from the epithelial fraction were sorted, incubated with 100 μg ovalbumin, and 20 μg/ml Poly(I:C) for 2 hr at 37°C, washed extensively, and incubated with CFSE-labeled OT-I cells in round bottom 96-well plates at a 1:5 ratio (10^4 DCs with 5 × 10^4 T cells). CFSE dilution was quantified 3 days later.

Immunohistology

For whole-mount preparations, the intestinal tissue was fixed with 10% paraformaldehyde (PFA) and immunostained according to standard procedure. For CD103 staining (Semmrich et al., 2012), mice were injected intraperitoneally with 10 μg of anti-CD103 PE. For IgA staining, the tissue was fixed with 2% PFA and cryosectioned.

In Vivo Uptake Assays

A ligate ileal loop was injected with 3–5 × 10^9 GFP-expressing *Salmonella* 3 × 10^9 beads or 100 μg of OVA-Alexa-594. Cells isolated from ileal segments were analyzed by flow cytometry 2–5 hr later. Some mice were intravenously (i.v.) injected with 400 μg/kg PTx 14–17 hr before *Salmonella* challenge (Huang et al., 2007; Fooksman et al., 2010).

Intravital 2-Photon Microscopy

Anesthetized mice were laparotomized. The ileum was externalized, immobilized, and cut open longitudinally using a cautery to be imaged using an Ultima 2-photon microscope (Prairie Technologies).

Supplementary Material

Refer to Web version on PubMed Central for supplementary material.

Acknowledgments

We thank Oliver Pabst and Steffen Jung for critical discussion, Mary Jo Wick and Wolf-Dietrich Hardt for providing *Salmonella* strains, and Olga Schultz for technical advice. This work was supported by the Leona M. and Harry B. Helmsley Charitable Trust and by the “NanoII” grant (#NMP4-LA-2009-229289) from the European Union FP7 program.

References

Abreu MT. Toll-like receptor signalling in the intestinal epithelium: how bacterial recognition shapes intestinal function. Nat Rev Immunol. 2010; 10:131–144. [PubMed: 20098461]

Adachi O, Kawai T, Takeda K, Matsumoto M, Tsutsui H, Sakagami M, Nakanishi K, Akira S. Targeted disruption of the MyD88 gene results in loss of IL-1- and IL-18-mediated function. Immunity. 1998; 9:143–150. [PubMed: 9697844]

Anjuère F, Luci C, Lebens M, Rousseau D, Hervouet C, Milon G, Holmgren J, Ardavin C, Czerkinsky C. In vivo adjuvant-induced mobilization and maturation of gut dendritic cells after oral administration of cholera toxin. J Immunol. 2004; 173:5103–5111. [PubMed: 15470054]

Annacker O, Coombes JL, Malmstrom V, Uhlig HH, Bourne T, Johansson-Lindbom B, Agace WW, Parker CM, Powrie F. Essential role for CD103 in the T cell-mediated regulation of experimental colitis. J Exp Med. 2005; 202:1051–1061. [PubMed: 16216886]

Arques JL, Hautefort I, Ivory K, Bertelli E, Regoli M, Clare S, Hinton JC, Nicoletti C. Salmonella induces flagellin- and MyD88-dependent migration of bacteria-capturing dendritic cells into the gut lumen. Gastroenterology. 2009; 137:579–587. e1–2. [PubMed: 19375423]

Bogunovic M, Ginhoux F, Helft J, Shang L, Hashimoto D, Greter M, Liu K, Jakubzick C, Ingersoll MA, Leboeuf M, et al. Origin of the lamina propria dendritic cell network. Immunity. 2009; 31:513–525. [PubMed: 19733489]

Boller K, Vestweber D, Kemler R. Cell-adhesion molecule uvo-morulin is localized in the intermediate junctions of adult intestinal epithelial cells. J Cell Biol. 1985; 100:327–332. [PubMed: 3880756]

Bowe F, Heffron F. Isolation of Salmonella mutants defective for intracellular survival. Methods Enzymol. 1994; 236:509–526. [PubMed: 7968635]

Brokaw JJ, White GW, Baluk P, Anderson GP, Umemoto EY, McDonald DM. Glucocorticoid-induced apoptosis of dendritic cells in the rat tracheal mucosa. Am J Respir Cell Mol Biol. 1998; 19:598–605. [PubMed: 9761756]

Cepek KL, Shaw SK, Parker CM, Russell GJ, Morrow JS, Rimm DL, Brenner MB. Adhesion between epithelial cells and T lymphocytes mediated by E-cadherin and the alpha E beta 7 integrin. Nature. 1994; 372:190–193. [PubMed: 7969453]

Chieppa M, Rescigno M, Huang AY, Germain RN. Dynamic imaging of dendritic cell extension into the small bowel lumen in response to epithelial cell TLR engagement. J Exp Med. 2006; 203:2841–2852. [PubMed: 17145958]

Coombes JL, Powrie F. Dendritic cells in intestinal immune regulation. Nat Rev Immunol. 2008; 8:435–446. [PubMed: 18500229]

Coombes JL, Siddiqui KR, Arancibia-Cárcamo CV, Hall J, Sun CM, Belkaid Y, Powrie F. A functionally specialized population of mucosal CD103+ DCs induces Foxp3+ regulatory T cells

via a TGF-beta and retinoic acid-dependent mechanism. J Exp Med. 2007; 204:1757–1764. [PubMed: 17620361]

Cruickshank SM, Deschoolmeester ML, Svensson M, Howell G, Bazakou A, Logunova L, Little MC, English N, Mack M, Grencis RK, et al. Rapid dendritic cell mobilization to the large intestinal epithelium is associated with resistance to Trichuris muris infection. J Immunol. 2009; 182:3055–3062. [PubMed: 19234202]

Diehl, GE.; Longman, RS.; Zhang, JX.; Breart, B.; Galan, C.; Cuesta, A.; Schwab, SR.; Littman, DR. Microbiota restricts trafficking of bacteria to mesenteric lymph nodes by CX_3CR1^{hi} cells. Nature. 2013. Published online January 13, 2013, http://dx.doi.org/10.1038/nature11809

Fooksman DR, Schwickert TA, Victora GD, Dustin ML, Nussenzweig MC, Skokos D. Development and migration of plasma cells in the mouse lymph node. Immunity. 2010; 33:118–127. [PubMed: 20619695]

Fujimoto K, Karuppuchamy T, Takemura N, Shimohigoshi M, Machida T, Haseda Y, Aoshi T, Ishii KJ, Akira S, Uematsu S. A new subset of CD103+CD8alpha+ dendritic cells in the small intestine expresses TLR3, TLR7, and TLR9 and induces Th1 response and CTL activity. J Immunol. 2011; 186:6287–6295. [PubMed: 21525388]

Halle S, Bumann D, Herbrand H, Willer Y, Dähne S, Förster R, Pabst O. Solitary intestinal lymphoid tissue provides a productive port of entry for Salmonella enterica serovar Typhimurium. Infect Immun. 2007; 75:1577–1585. [PubMed: 17283101]

Hapfelmeier S, Stecher B, Barthel M, Kremer M, Müller AJ, Heikenwalder M, Stallmach T, Hensel M, Pfeffer K, Akira S, Hardt WD. The Salmonella pathogenicity island (SPI)-2 and SPI-1 type III secretion systems allow Salmonella serovar typhimurium to trigger colitis via MyD88-dependent and MyD88-independent mechanisms. J Immunol. 2005; 174:1675–1685. [PubMed: 15661931]

Hebel K, Griewank K, Inamine A, Chang HD, Müller-Hilke B, Fillatreau S, Manz RA, Radbruch A, Jung S. Plasma cell differentiation in T-independent type 2 immune responses is independent of CD11c(high) dendritic cells. Eur J Immunol. 2006; 36:2912–2919. [PubMed: 17051619]

Hermiston ML, Gordon JI. In vivo analysis of cadherin function in the mouse intestinal epithelium: essential roles in adhesion, maintenance of differentiation, and regulation of programmed cell death. J Cell Biol. 1995; 129:489–506. [PubMed: 7721948]

Huang JH, Cárdenas-Navia LI, Caldwell CC, Plumb TJ, Radu CG, Rocha PN, Wilder T, Bromberg JS, Cronstein BN, Sitkovsky M, et al. Requirements for T lymphocyte migration in explanted lymph nodes. J Immunol. 2007; 178:7747–7755. [PubMed: 17548612]

Huleatt JW, Lefrançois L. Antigen-driven induction of CD11c on intestinal intraepithelial lymphocytes and CD8+ T cells in vivo. J Immunol. 1995; 154:5684–5693. [PubMed: 7751620]

Iliev ID, Mileti E, Matteoli G, Chieppa M, Rescigno M. Intestinal epithelial cells promote colitis-protective regulatory T-cell differentiation through dendritic cell conditioning. Mucosal Immunol. 2009; 2:340–350. [PubMed: 19387433]

Iwata M, Hirakiyama A, Eshima Y, Kagechika H, Kato C, Song SY. Retinoic acid imprints gut-homing specificity on T cells. Immunity. 2004; 21:527–538. [PubMed: 15485630]

Izadpanah A, Dwinell MB, Eckmann L, Varki NM, Kagnoff MF. Regulated MIP-3alpha/CCL20 production by human intestinal epithelium: mechanism for modulating mucosal immunity. Am J Physiol Gastrointest Liver Physiol. 2001; 280:G710–G719. [PubMed: 11254498]

Jaensson E, Uronen-Hansson H, Pabst O, Eksteen B, Tian J, Coombes JL, Berg PL, Davidsson T, Powrie F, Johansson-Lindbom B, Agace WW. Small intestinal CD103+ dendritic cells display unique functional properties that are conserved between mice and humans. J Exp Med. 2008; 205:2139–2149. [PubMed: 18710932]

Jang MH, Kweon MN, Iwatani K, Yamamoto M, Terahara K, Sasakawa C, Suzuki T, Nochi T, Yokota Y, Rennert PD, et al. Intestinal villous M cells: an antigen entry site in the mucosal epithelium. Proc Natl Acad Sci USA. 2004; 101:6110–6115. [PubMed: 15071180]

Jang MH, Sougawa N, Tanaka T, Hirata T, Hiroi T, Tohya K, Guo Z, Umemoto E, Ebisuno Y, Yang BG, et al. CCR7 is critically important for migration of dendritic cells in intestinal lamina propria to mesenteric lymph nodes. J Immunol. 2006; 176:803–810. [PubMed: 16393963]

Johansson-Lindbom B, Svensson M, Pabst O, Palmqvist C, Marquez G, Förster R, Agace WW. Functional specialization of gut CD103+ dendritic cells in the regulation of tissue-selective T cell homing. J Exp Med. 2005; 202:1063–1073. [PubMed: 16216890]

Jones BD, Ghori N, Falkow S. Salmonella typhimurium initiates murine infection by penetrating and destroying the specialized epithelial M cells of the Peyer's patches. J Exp Med. 1994; 180:15–23. [PubMed: 8006579]

Jung S, Aliberti J, Graemmel P, Sunshine MJ, Kreutzberg GW, Sher A, Littman DR. Analysis of fractalkine receptor CX(3)CR1 function by targeted deletion and green fluorescent protein reporter gene insertion. Mol Cell Biol. 2000; 20:4106–4114. [PubMed: 10805752]

Kinnebrew MA, Buffie CG, Diehl GE, Zenewicz LA, Leiner I, Hohl TM, Flavell RA, Littman DR, Pamer EG. Interleukin 23 production by intestinal CD103(+)CD11b(+) dendritic cells in response to bacterial flagellin enhances mucosal innate immune defense. Immunity. 2012; 36:276–287. [PubMed: 22306017]

Laffont S, Siddiqui KR, Powrie F. Intestinal inflammation abrogates the tolerogenic properties of MLN CD103+ dendritic cells. Eur J Immunol. 2010; 40:1877–1883. [PubMed: 20432234]

Le Borgne M, Etchart N, Goubier A, Lira SA, Sirard JC, van Rooijen N, Caux C, Aït-Yahia S, Vicari A, Kaiserlian D, Dubois B. Dendritic cells rapidly recruited into epithelial tissues via CCR6/CCL20 are responsible for CD8+ T cell crosspriming in vivo. Immunity. 2006; 24:191–201. [PubMed: 16473831]

Lindquist RL, Shakhar G, Dudziak D, Wardemann H, Eisenreich T, Dustin ML, Nussenzweig MC. Visualizing dendritic cell networks in vivo. Nat Immunol. 2004; 5:1243–1250. [PubMed: 15543150]

Mach N, Gillessen S, Wilson SB, Sheehan C, Mihm M, Dranoff G. Differences in dendritic cells stimulated in vivo by tumors engineered to secrete granulocyte-macrophage colony-stimulating factor or Flt3-ligand. Cancer Res. 2000; 60:3239–3246. [PubMed: 10866317]

Mackarehtschian K, Hardin JD, Moore KA, Boast S, Goff SP, Lemischka IR. Targeted disruption of the flk2/flt3 gene leads to deficiencies in primitive hematopoietic progenitors. Immunity. 1995; 3:147–161. [PubMed: 7621074]

Maric I, Holt PG, Perdue MH, Bienenstock J. Class II MHC antigen (Ia)-bearing dendritic cells in the epithelium of the rat intestine. J Immunol. 1996; 156:1408–1414. [PubMed: 8568241]

McDole JR, Wheeler LW, McDonald KG, Wang B, Konjufca V, Knoop KA, Newberry RD, Miller MJ. Goblet cells deliver luminal antigen to CD103+ dendritic cells in the small intestine. Nature. 2012; 483:345–349. [PubMed: 22422267]

McDonald KG, Leach MR, Brooke KWM, Wang C, Wheeler LW, Hanly EK, Rowley CW, Levin MS, Wagner M, Li E, Newberry RD. Epithelial expression of the cytosolic retinoid chaperone cellular retinol binding protein II is essential for in vivo imprinting of local gut dendritic cells by lumenal retinoids. Am J Pathol. 2012; 180:984–997. [PubMed: 22222225]

Mucida D, Park Y, Kim G, Turovskaya O, Scott I, Kronenberg M, Cheroutre H. Reciprocal TH17 and regulatory T cell differentiation mediated by retinoic acid. Science. 2007; 317:256–260. [PubMed: 17569825]

Nakano H, Yanagita M, Gunn MD. CD11c(+)B220(+)Gr-1(+) cells in mouse lymph nodes and spleen display characteristics of plasmacytoid dendritic cells. J Exp Med. 2001; 194:1171–1178. [PubMed: 11602645]

Niess JH, Brand S, Gu X, Landsman L, Jung S, McCormick BA, Vyas JM, Boes M, Ploegh HL, Fox JG, et al. CX3CR1-mediated dendritic cell access to the intestinal lumen and bacterial clearance. Science. 2005; 307:254–258. [PubMed: 15653504]

Parker CM, Cepek KL, Russell GJ, Shaw SK, Posnett DN, Schwarting R, Brenner MB. A family of beta 7 integrins on human mucosal lymphocytes. Proc Natl Acad Sci USA. 1992; 89:1924–1928. [PubMed: 1542691]

Persson EK, Jaensson E, Agace WW. The diverse ontogeny and function of murine small intestinal dendritic cell/macrophage subsets. Immunobiology. 2010; 215:692–697. [PubMed: 20580119]

Rescigno M. Intestinal dendritic cells. Adv Immunol. 2010; 107:109–138. [PubMed: 21034972]

Rescigno M, Urbano M, Valzasina B, Francolini M, Rotta G, Bonasio R, Granucci F, Kraehenbuhl JP, Ricciardi-Castagnoli P. Dendritic cells express tight junction proteins and penetrate gut epithelial monolayers to sample bacteria. Nat Immunol. 2001; 2:361–367. [PubMed: 11276208]

Rivollier A, He J, Kole A, Valatas V, Kelsall BL. Inflammation switches the differentiation program of Ly6Chi monocytes from antiinflammatory macrophages to inflammatory dendritic cells in the colon. J Exp Med. 2012; 209:139–155. [PubMed: 22231304]

Schlickum S, Sennefelder H, Friedrich M, Harms G, Lohse MJ, Kilshaw P, Schön MP. Integrin α E(CD103)β 7 influences cellular shape and motility in a ligand-dependent fashion. Blood. 2008; 112:619–625. [PubMed: 18492951]

Schödel F, Kelly SM, Peterson DL, Milich DR, Curtiss R 3rd. Hybrid hepatitis B virus core-pre-S proteins synthesized in avirulent Salmonella typhimurium and Salmonella typhi for oral vaccination. Infect Immun. 1994; 62:1669–1676. [PubMed: 8168928]

Schulz O, Jaensson E, Persson EK, Liu X, Worbs T, Agace WW, Pabst O. Intestinal CD103+, but not CX3CR1+, antigen sampling cells migrate in lymph and serve classical dendritic cell functions. J Exp Med. 2009; 206:3101–3114. [PubMed: 20008524]

Scott CL, Aumeunier AM, Mowat AM. Intestinal CD103+ dendritic cells: master regulators of tolerance? Trends Immunol. 2011; 32:412–419. [PubMed: 21816673]

Semmrich M, Plantinga M, Svensson-Frej M, Uronen-Hansson H, Gustafsson T, Mowat AM, Yrlid U, Lambrecht BN, Agace WW. Directed antigen targeting in vivo identifies a role for CD103+ dendritic cells in both tolerogenic and immunogenic T-cell responses. Mucosal Immunol. 2012; 5:150–160. [PubMed: 22166938]

Sun CM, Hall JA, Blank RB, Bouladoux N, Oukka M, Mora JR, Belkaid Y. Small intestine lamina propria dendritic cells promote de novo generation of Foxp3 T reg cells via retinoic acid. J Exp Med. 2007; 204:1775–1785. [PubMed: 17620362]

Sung SS, Fu SM, Rose CE Jr, Gaskin F, Ju ST, Beaty SR. A major lung CD103 (alphaE)-beta7 integrin-positive epithelial dendritic cell population expressing Langerin and tight junction proteins. J Immunol. 2006; 176:2161–2172. [PubMed: 16455972]

Takahashi-Iwanaga H, Iwanaga T, Isayama H. Porosity of the epithelial basement membrane as an indicator of macrophage-enterocyte interaction in the intestinal mucosa. Arch Histol Cytol. 1999; 62:471–481. [PubMed: 10678576]

Tal O, Lim HY, Gurevich I, Milo I, Shipony Z, Ng LG, Angeli V, Shakhar G. DC mobilization from the skin requires docking to immobilized CCL21 on lymphatic endothelium and intralymphatic crawling. J Exp Med. 2011; 208:2141–2153. [PubMed: 21930767]

Uematsu S, Akira S. Immune responses of TLR5(+) lamina propria dendritic cells in enterobacterial infection. J Gastroenterol. 2009; 44:803–811. [PubMed: 19547909]

Uematsu S, Jang MH, Chevrier N, Guo Z, Kumagai Y, Yamamoto M, Kato H, Sougawa N, Matsui H, Kuwata H, et al. Detection of pathogenic intestinal bacteria by Toll-like receptor 5 on intestinal CD11c+ lamina propria cells. Nat Immunol. 2006; 7:868–874. [PubMed: 16829963]

Uematsu S, Fujimoto K, Jang MH, Yang BG, Jung YJ, Nishiyama M, Sato S, Tsujimura T, Yamamoto M, Yokota Y, et al. Regulation of humoral and cellular gut immunity by lamina propria dendritic cells expressing Toll-like receptor 5. Nat Immunol. 2008; 9:769–776. [PubMed: 18516037]

Vallon-Eberhard A, Landsman L, Yogev N, Verrier B, Jung S. Transepithelial pathogen uptake into the small intestinal lamina propria. J Immunol. 2006; 176:2465–2469. [PubMed: 16456006]

Varol C, Vallon-Eberhard A, Elinav E, Aychek T, Shapira Y, Luche H, Fehling HJ, Hardt WD, Shakhar G, Jung S. Intestinal lamina propria dendritic cell subsets have different origin and functions. Immunity. 2009; 31:502–512. [PubMed: 19733097]

Varol C, Zigmond E, Jung S. Securing the immune tightrope: mononuclear phagocytes in the intestinal lamina propria. Nat Rev Immunol. 2010; 10:415–426. [PubMed: 20498668]

Yamamoto M, Sato S, Hemmi H, Hoshino K, Kaisho T, Sanjo H, Takeuchi O, Sugiyama M, Okabe M, Takeda K, Akira S. Role of adaptor TRIF in the MyD88-independent toll-like receptor signaling pathway. Science. 2003; 301:640–643. [PubMed: 12855817]

Yrlid U, Svensson M, Håkansson A, Chambers BJJ, Ljunggren HGG, Wick MJJ. In vivo activation of dendritic cells and T cells during Salmonella enterica serovar Typhimurium infection. Infect Immun. 2001; 69:5726–5735. [PubMed: 11500449]

Zigmond E, Varol C, Farache J, Elmaliah E, Ansuman T, Friedlander G, Mack M, Shpigel N, Boneca IG. Ly6C hi monocytes in the inflamed colon give rise to proinflammatory effector cells and migratory antigen presenting cells. Immunity. 2012:1076–1090. [PubMed: 23219392]

Zimmerli SC, Hauser C. Langerhans cells and lymph node dendritic cells express the tight junction component claudin-1. J Invest Dermatol. 2007; 127:2381–2390. [PubMed: 17508021]

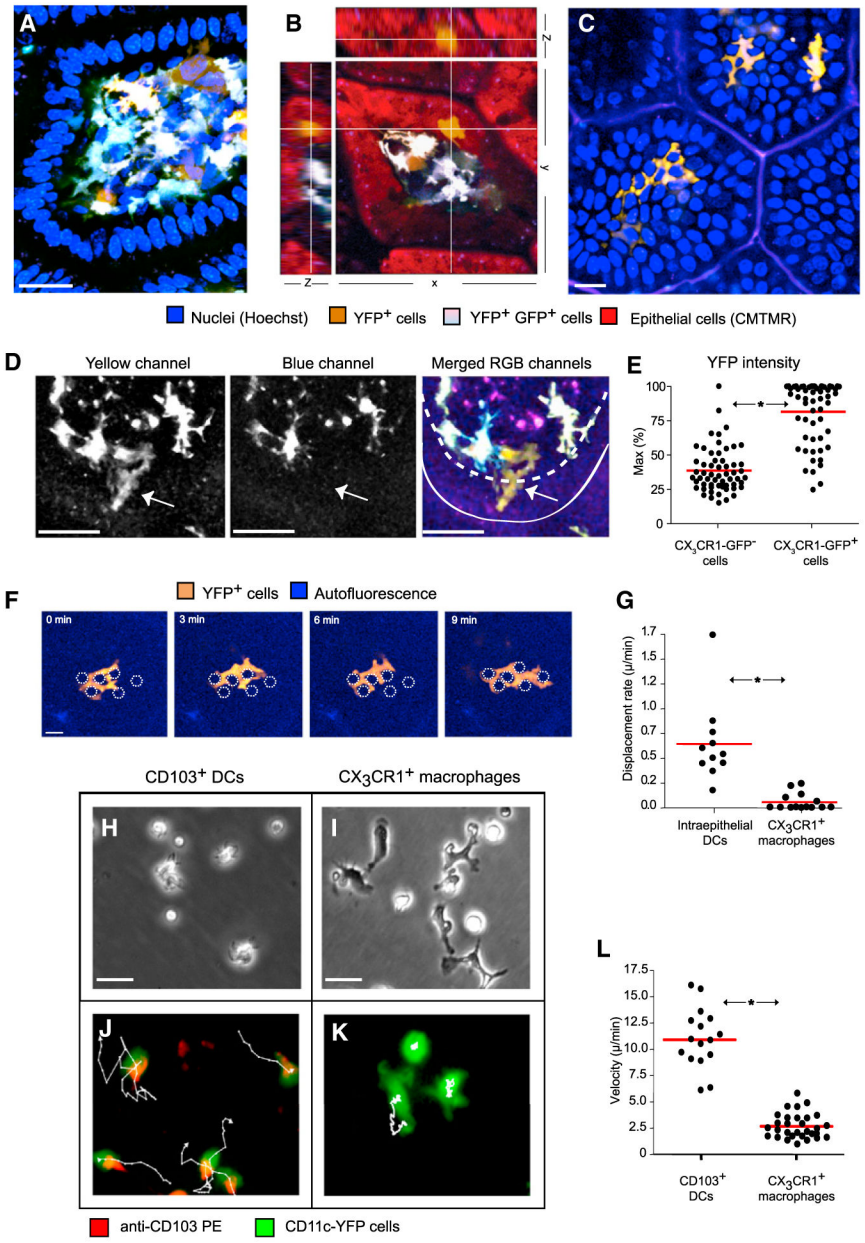

Figure 1. A Population of Motile CX$_3$CR1-GFP$^-$CD11c-YFP^{int} Cells Occupies the Intestinal Epithelium

Two-photon microscopy in the ileum of a live Cx$_3$cr1$^{+/gfp}$ × Cd11c-YFP mice.

(A) A cross-section through a villus; the LP is populated by sparse GFP$^-$YFP^{int} cells and abundant GFP$^+$YFP^{hi} cells, whose exact hue depends on the ratio of GFP to YFP (scale bar represents 25 μM).

(B) Examining reconstructed data from three axes highlights a GFP$^-$YFP^{int} cell lodged within the epithelial layer.

(C) A cross-section through the apical epithelium of several adjacent villi shows 3 GFP$^-$YFP^{int} cells occupying the space between epithelial cells (scale bar represents 25 μM).

(D) A $GFP^{-}YFP^{int}$cell (arrow) fluoresces in the yellow channel but not the blue channel. Solid and dashed lines outline the luminal surface and basement membrane, respectively. (A–D, data are representative of at least 20 independent experiments).

(E) In 2-photon microscopy, large motile amoeboid CX_3CR1-GFP^{-} cells showed on average half the YFP intensity as $CX_3CR1^{-}GFP^{+}$ cells (horizontal bars denote averages, $p < 0.0001$, $n = 65$, five independent experiments).

(F) A YFP^{int} cell was followed in the epithelium for 9 min. The cell meandered between enterocytes, whose inferred positions are indicated by white polygons, without displacing them (scale bar represents 30 μM).

(G) Based on intravital 2-photon microscopy, the displacement rate of $CD103^{+}$ DCs was significantly ($p < 0.0001$) higher than of X_3CR1^{+} macrophages imaged in the same villi ($n = 27$, three independent experiments). In vitro live-cell microscopy of $CD103^{+}$ DCs (H and J) and CX_3CR1^{+} macrophages (I and K) sorted using flow cytometry from the LP revealed their intrinsic motility patterns (scale bars represent 30 μM).

(H) $CD103^{+}$ DCs displayed amoeboid morphology.

(I) CX_3CR1^{+} macrophages adhered to the plate showing stellate morphology.

(J) $CD103^{+}$ DCs crawled vigorously, using lamellipodia at the leading edge and trailing a distinct $CD103^{-}$rich uropod; tracks follow 3 cells for 30 min.

(K) Similarly tracked CX_3CR1^{+} macrophages displayed little lateral displacement.

(L) Image analysis demonstrate that, in vitro, $CD103^{+}$ DCs crawled four times faster than CX_3CR1^{+} macrophages ($n = 50$, $p < 0.000.1$, horizontal bars denote averages, representative of three independent experiments).

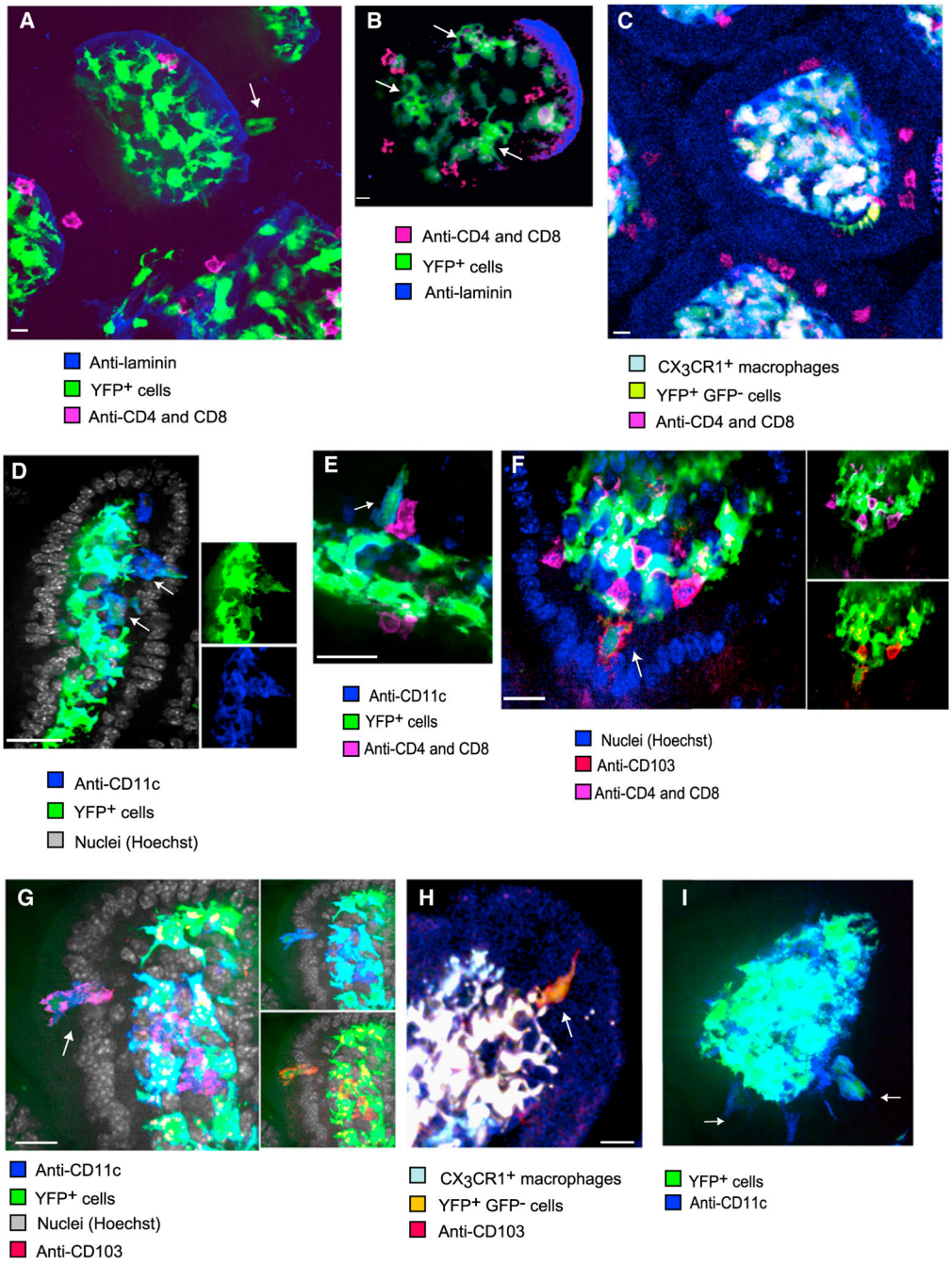

Figure 2. Immunohistology of the Epithelium Identifies CD11c-YFP^{int} Cells as CD103^{+} DCs

Samples of the small intestine from untreated mice were rapidly excised and fixed for immunohistological analysis of whole-mounted tissues. Single Z-planes are shown (scale bars represent 10 μM).

(A) In *Cd11c*-YFP mice, not only CD4^{+}CD8^{+} IELs but also some CD11c-YFP^{+} cells (arrow) were located directly above the laminin^{+} basement membrane among enterocytes. Such cells expressed less YFP than the highly-branched cells confined to the LP.

(B) Within the epithelial layer, amoeboid YFP^{+} cells (arrows) could be seen alongside IELs.

(C) A $CX_3CR1\text{-}GFP^{-}CD11c\text{-}YFP^{+}$ cell (in yellow) in the epithelium exhibited an elaborate shape and no T cell markers

(D) YFP^{int} cells (arrows), located beneath and among enterocytes expressed membranal CD11c.

(E) A YFP^{int} cell (arrow) expresses CD11c, but not CD4 or CD8, whereas adjacent IELs do.

(F) CD103 is expressed by the large YFP^{+} cells (arrow), which do not express CD4 or CD8.

(G) CD103 and CD11c are coexpressed by a large YFP^{+} cell (arrow) in the epithelium.

(H) $CX_3CR1^{-}GFP^{-}CD11c\text{-}YFP^{int}$ cells, marked with membranal $CD103^{+}$, can be located in the epithelium.

(I) YFP^{+} $CD11c^{+}$ cells were also observed in the epithelium of *Rag1*$^{-/-}$ mice (arrows). All micrographs are representative of at least six independent samples.

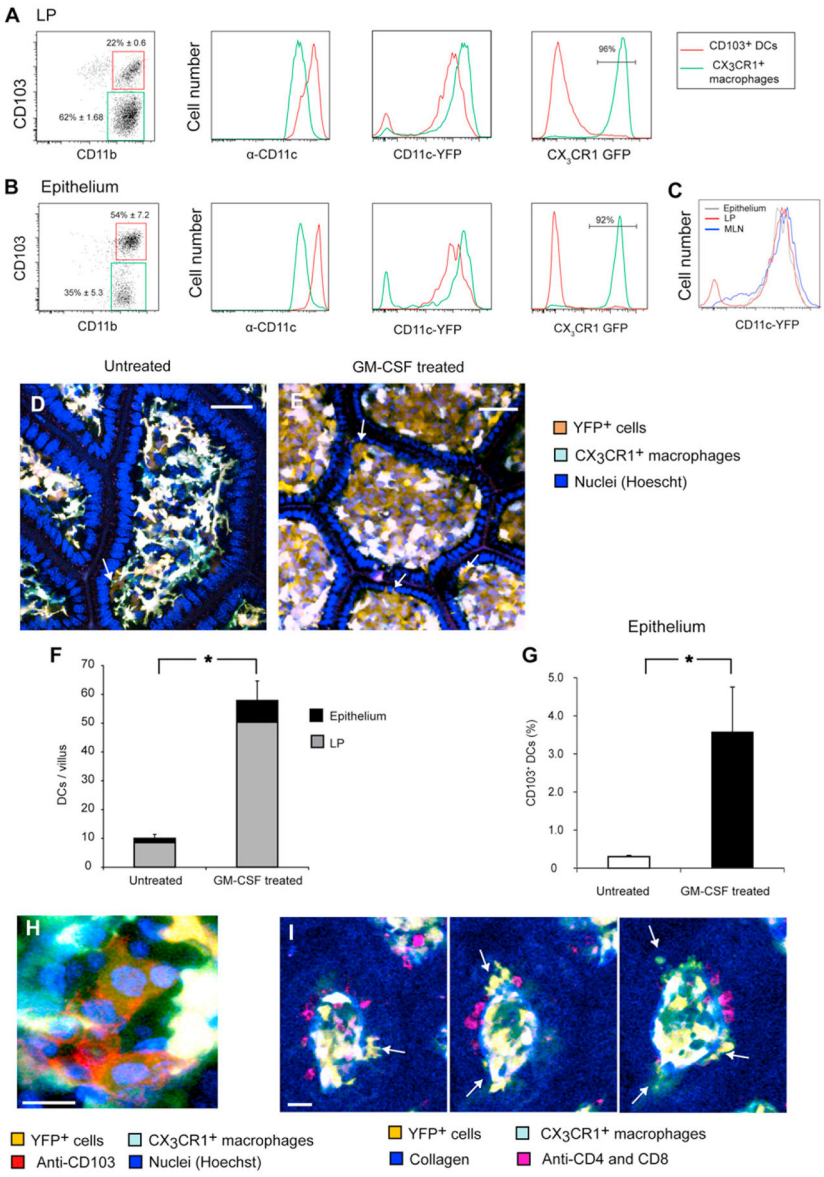

Figure 3. CX_3CR1-GFP$^-$CD11c-YFP^{int} Cells Are CD103$^+$ DCs Responsive to GM-CSF

(A and B) Following separation of the ileal tissue to the LP (A) and intraepithelial compartment (B), live MHC-II$^+$ CD11c$^+$ cells were analyzed by flow cytometry as detailed in Figure S1. Data are representative of at least five independent experiments. (A) In the LP, CX_3CR1^+ macrophages outnumbered CD103$^+$ DCs 3- to 4-fold (left). Even though CD103$^+$ DCs expressed more membranal CD11c (center left), they showed less YFP fluorescence (center right). (B) In the epithelium, CD103$^+$ DCs dominated, although contaminant CX_3CR1^+ cells from the LP were also detectable. A similar relation between YFP and CD11c was observed.

(C) MHC-II$^+$CD11b$^+$CD11c$^+$CD103$^+$ DCs from the epithelium showed the same YFP intensity as did CD103$^+$ DCs in the LP and MLN.

(D–I) GM-CSF specifically expanded GFP$^-$YFP^{int} cells. Using 2-photon microscopy, we compared untreated *Cx3cr1*$^{+/gfp}$ × *Cd11c*-YFP mice (D) with mice inoculated with a GM-

CSF-secreting tumor (E). Arrows point to DCs in the epithelium (scale bar represents 50 μM). (F) GM-CSF expanded $GFP^{-}YFP^{int}$ cells 6-fold ($p < 0.0001$) in both the LP and epithelium, while $GFP^{+}YFP^{hi}$ cells were not affected noticeably (16 villi from two experiments, error bars indicate SEM for total numbers). (G) Flow cytometry analysis confirmed the proliferation of $CD103^{+}$ DCs in the epithelium. Columns depict the percentages of $CD103^{+}$ DCs out of hematopoietic cells based on data pooled from three experiments. (H) Whole-mount immunohistology confirmed that $GFP^{-}YFP^{int}$ cells in GM-CSF-treated mice expressed membranal CD103 (scale bars represent 10 μM). (I) Serial Z sections through a villus in a GM-CSF-treated mouse show multiple $CX_3CR1\text{-}GFP^{-}$ $CD11c\text{-}YFP^{int}$ cells (arrows), which did not express CD4 or CD8 markers (scale bars represent 30 μM). Images are representative of two experiments.

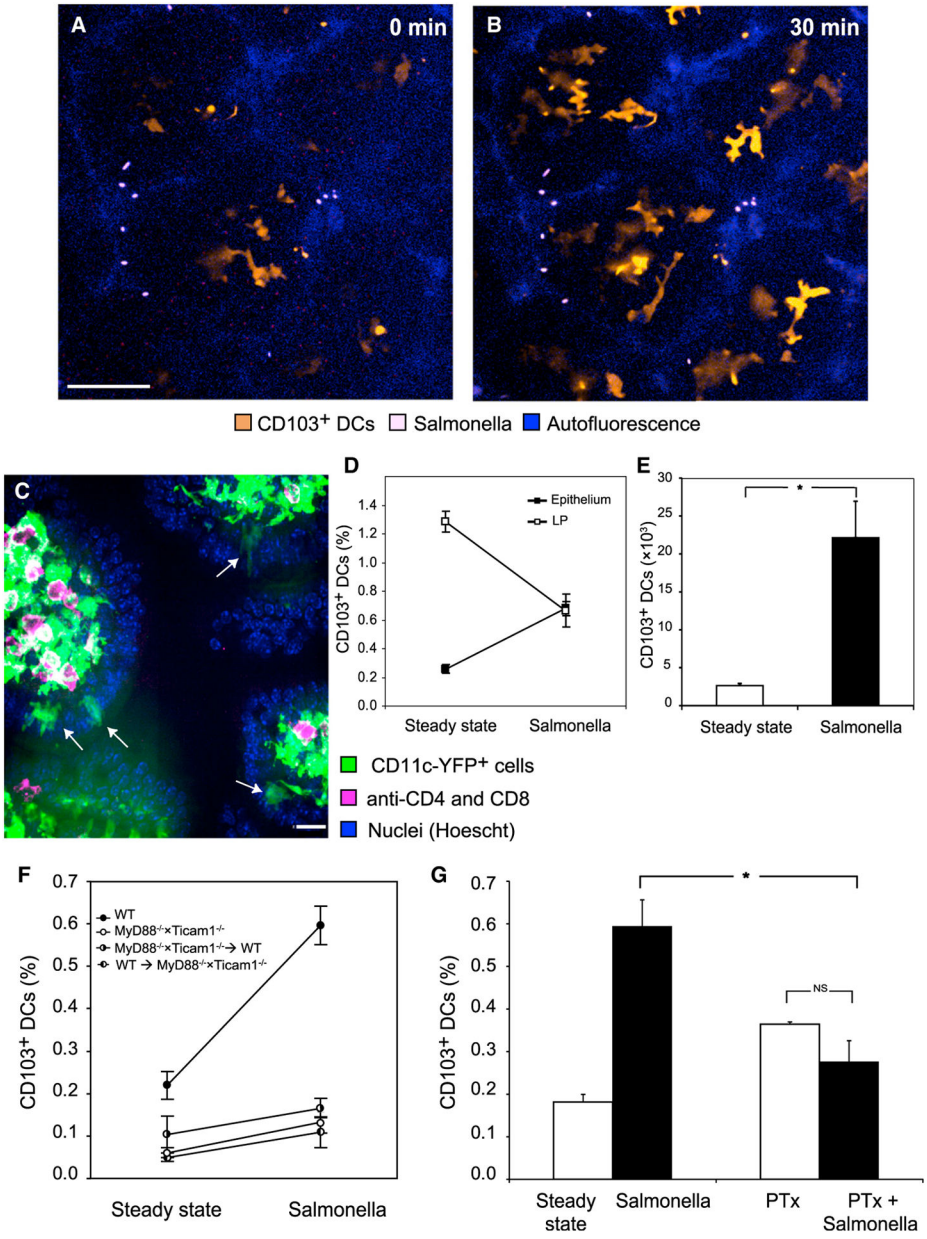

Figure 4. Luminal *Salmonella* Recruit CD103$^+$ DCs to the Epithelium

(A and B) Two-photon microscopy of the epithelial layer in several adjacent villi exposed to *Salmonella*. (A) Some intraepithelial YFP^{int} CD103$^+$ DCs were already visible at time 0, but within 30 min (B) they were joined by several other DCs that had migrated up into the epithelium (scale bar represents 50 μM).

(C) Immunohistology following *Salmonella* challenge captured several CD103$^+$ DCs (arrows) within the epithelium. Image is representative of three experiments.

(D and E) By flow cytometry, *Salmonella* challenge increased the percentage of CD103$^+$ DCs in the epithelium ($p < 0.0001$) and concomitantly decreased it in the LP ($p = 0.003$, data pooled from four experiments; percentages of DCs were calculated out of total live cells).

(E) This translated to a marked increase in the total number of $CD103^+$ DCs in the epithelium ($p < 0.0001$).

(F) We examined the ileal epithelium of WT mice, mice deficient in MyD88 and *Ticam1* (TRIF) and chimeric mice whose hematopoietic cells are either $MyD88^{-/-} \times Ticam1^{-/-}$ or WT. $Myd88^{-/-} \times Ticam1^{-/-}$ mice had significantly lower percentages of intraepithelial $CD103^+$ DCs ($p = 0.012$) and only in WT mice did *Salmonella* challenge significantly recruit $CD103^+$ DCs, as indicated by ANOVA ($p < 0.001$, $n = 27$, data were pooled from two experiments and percentages calculated out of total live cells).

(G) Overnight treatment of mice with PTx significantly reduced the recruitment of $CD103^+$ DCs to the epithelium (significant interaction at $p < 0.001$, $n = 18$, data pooled from two experiments). Error bars indicate SEM. Columns depict the percentages of $CD103^+$ DCs out of total live cells.

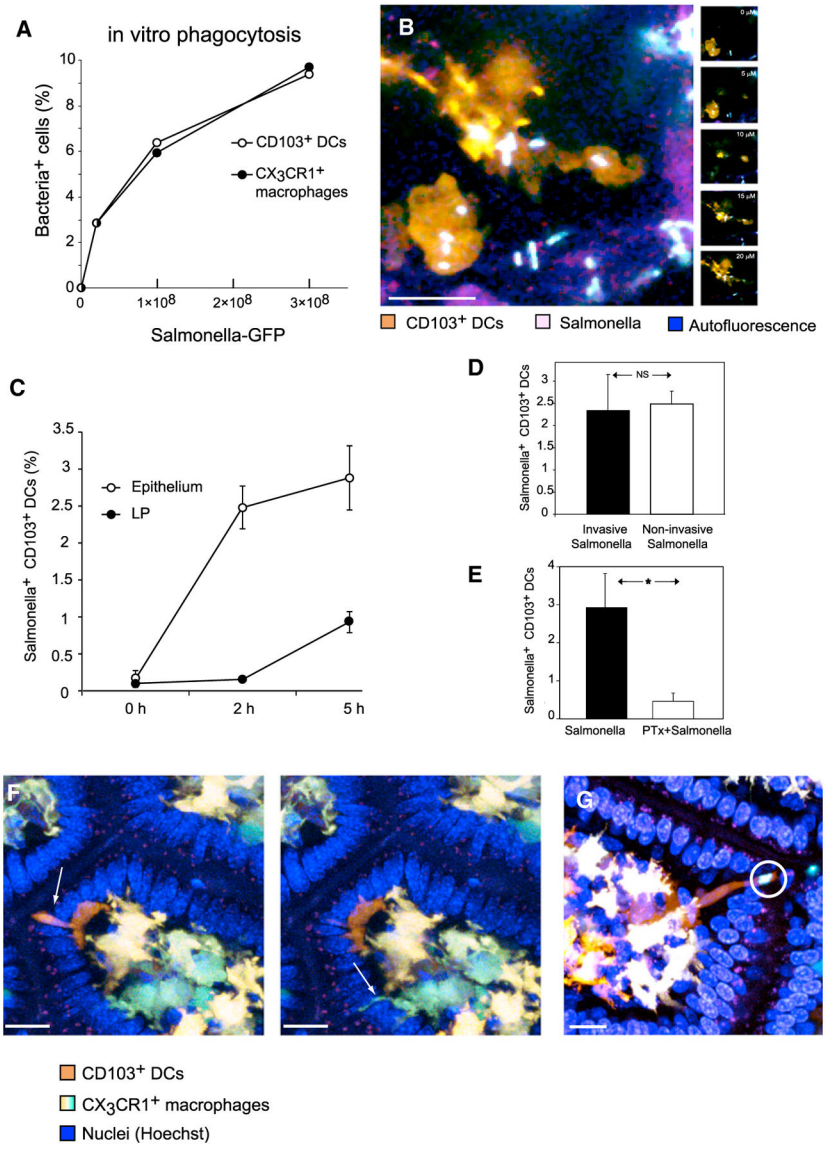

Figure 5. *Salmonella* Uptake by CD103$^+$ DCs Is Active and Chemokine-Dependent

(A) We incubated 2 × 10^6 cells containing all subsets of mononuclear phagocytes from the LP with increasing numbers of GFP$^+$ *Salmonella*. CD103$^+$ DCs were as efficient as CX_3CR1^+ macrophages at ingesting *Salmonella* (representative of two experiments).

(B) After applying *Salmonella* to the ileal lumen, 2-photon microscopy could visualize GFP$^+$ bacteria accumulating, within 30 min, inside intraepithelial CD103$^+$ DCs (maximum intensity projection, left). Individual Z-planes (depths indicated) show that bacteria were internalized.

(C–E) Ileal loops were injected with GFP$^+$ *Salmonella*. In vivo bacterial sampling by intestinal CD103$^+$ DCs was assessed by flow cytometry. Error bars indicate SEM (C) CD103$^+$ DCs in the epithelium were the first to capture *Salmonella*: by 2 hr, 2.5% the DCs in this compartment became GFP$^+$, whereas no ingestion was detected in the LP. At 5 hr, bacteria further accumulated in intra-epithelial DCs but were also detected in DCs in the LP.

(D) Intestines were injected with the invasive *Salmonella* strain χ4550 or with the noninvasive strain SB161. Both strains were sampled as efficiently by $CD103^+$ DCs isolated from the epithelium at 2 hr (n = 13, data pooled from two experiments). (E) Overnight treatment of mice with PTx almost ablated *Salmonella* uptake at 2 hr ($p < 0.0001$, n = 18, two combined experiments).

(F) As $CD103^+$ DCs crawl above the basement membrane, they extend dendrites through the epithelium (arrow on left). These extensions are thicker than the TEDs extended by CX_3CR1^+ macrophages (arrow on right). Data are representative of at least ten independent experiments.

(G) In several instances, the dendrites of $CD103^+$ DCs could be seen engulfing *Salmonell*a (two bacteria circled), and retracting them toward their soma (scale bar represents 20 μM).

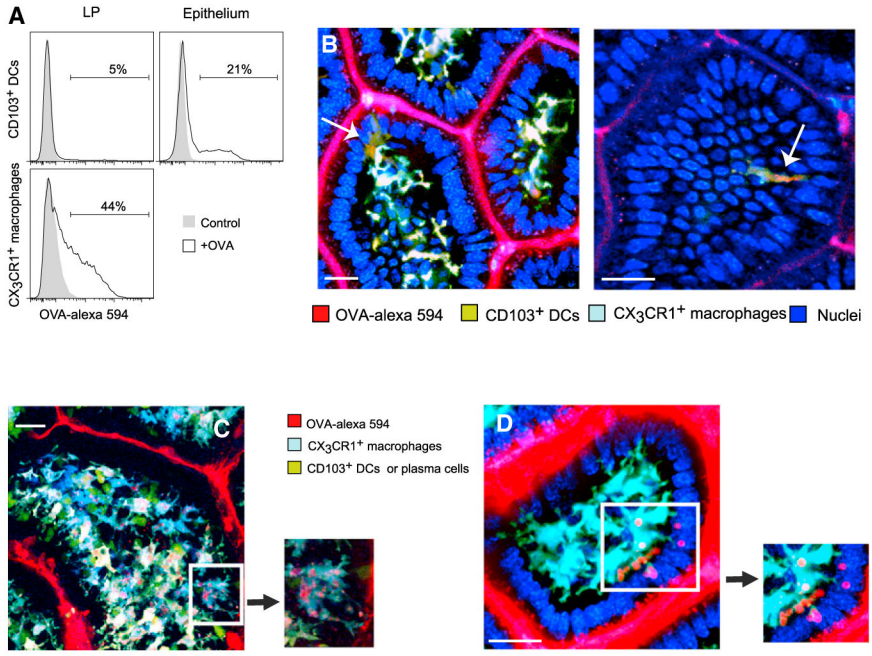

Figure 6. CD103$^+$ DCs in the Epithelium Sample Soluble Ag

(A) The ligated ileum was injected with Alexa-549-OVA and harvested at 2 hr to assess Ag uptake by MHCII$^+$CD11c$^+$ mononuclear phagocytes in the LP and epithelium using flow cytometry. Although CD103$^+$ DCs in the LP failed to ingest OVA (top left), significantly more ($p < 0.002$) DCs in the epithelium could ingest it (top right). CX_3CR1^+ macrophages in the LP (bottom) were significantly more efficient at ingesting OVA. Data are representative of three independent experiments.

(B and C) Two-photon microscopy of a *Cx$_3$cr1*-GFP ×*Cd11c*-YFP mouse 20 min after Alexa-549-OVA was applied to the mucosa (scale bar represents 20 μM). (B) CD103$^+$ DCs in the epithelium extend dendrites and accumulate Ag inclusions (arrows). (C) Most CX_3CR1^+ macrophages accumulate OVA in vacuoles. Ag uptake was not confined to macrophages contacting the epithelium. Ovoid CD11c-YFP^{hi} plasma cells are also visible. In the insets, OVA$^+$ vesicles propagate along macrophages TEDs.

(D) OVA$^+$ vacuoles are engulfed by macrophage membranes. The scale bar represents 30 μM; images are representative of at least five independent experiments.

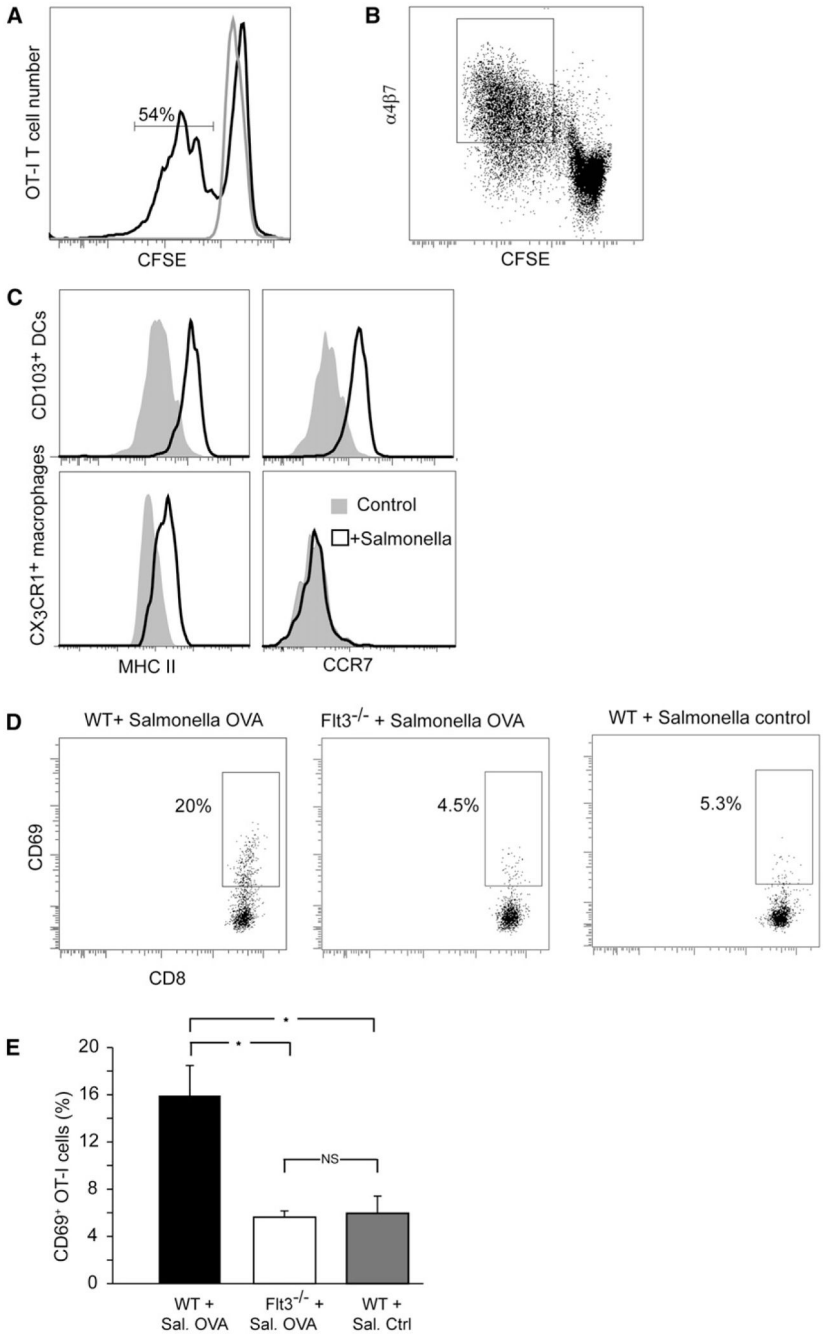

Figure 7. CD103$^+$ DCs from the Epithelium Are Capable APCs, and Their Absence Impairs T Cell Activation

(A and B) CD103$^+$ DCs, either pulsed with OVA or used as controls were cocultured with CSFE-labeled OT-I CD8$^+$ T cells. At 3 days, 54% of T cells have proliferated (A) and upregulated the gut-tropic α4β7 integrin (B). (A) and (B) are representative of three independent experiments.

(C) Following in vitro exposure to *Salmonella* for 5 hr, both CD103$^+$ DCs and CX_3CR1^+ macrophages upregulated MHC-II but only CD103$^+$ DCs also upregulated CCR7 (is representative of two independent experiments).

(D) WT and *Flt3*$^{-/-}$ mice were transferred i.v. with OT-I cells and inoculated with WT or OVA^{+} *Salmonella* in the gut. Analysis of CD69 expression in MLNs 40 hr later showed Ag-specific activation of OT-I T cells in WT ($p < 0.001$) but not *Flt3*$^{-/-}$ ($p = 0.84$, $n = 8$) mice compared to the response to WT *Salmonella*, as quantified in (E). Error bars represent SEM.